

Assessing groundwater quality in Greece based on spatial and temporal analysis

Zoi Dokou · Nektarios N. Kourgiyas ·
George P. Karatzas

Received: 5 May 2015 / Accepted: 20 November 2015 / Published online: 26 November 2015
© Springer International Publishing Switzerland 2015

Abstract The recent industrial growth together with the urban expansion and intensive agriculture in Greece has increased groundwater contamination in many regions of the country. In order to design successful remediation strategies and protect public health, it is very important to identify those areas that are most vulnerable to groundwater contamination. In this work, an extensive contamination database from monitoring wells that cover the entire Greek territory during the last decade (2000–2008) was used in order to study the temporal and spatial distribution of groundwater contamination for the most common and serious anionic and cationic trace element pollutants (heavy metals). Spatial and temporal patterns and trends in the occurrence of groundwater contamination were also identified highlighting the regions where the higher groundwater contamination rates have been detected across the country. As a next step, representative contaminated aquifers in Greece, which were identified by the above analysis, were selected in order to analyze the specific contamination problem in more detail. To this end, geostatistical techniques (various types of kriging, co-kriging, and indicator kriging) were employed in order to map the contaminant values and the probability of exceeding

critical thresholds (set as the parametric values of the contaminant of interest in each case). The resulting groundwater contamination maps could be used as a useful tool for water policy makers and water managers in order to assist the decision-making process.

Keywords Groundwater contamination · Major ions · Heavy metals · Kriging · Geostatistics

Introduction

Water resources worldwide are currently under an increasing pressure due mainly to the urban expansion that, together with the high population density and industrial development, has resulted in an increase in water demand and at the same time has contributed significantly to the contamination of the existing water bodies. Greece is no exception to water-related problems. Groundwater systems in Greece experience significant pressure on their quantity, due to increased water abstraction and lowering of the water levels, and their quality, related to pollution from point and non-point sources.

A wide variety of materials have been identified as contaminants found in groundwater such as organic and inorganic compounds, pathogens, heavy metals, and hydrocarbons. The most common contamination problems encountered in Greece are seawater intrusion, nitrate pollution caused by intensive agriculture activities, and heavy metal contamination, especially near mines or industrial areas. Saltwater intrusion is a problem that

Electronic supplementary material The online version of this article (doi:10.1007/s10661-015-4998-0) contains supplementary material, which is available to authorized users.

Z. Dokou (✉) · N. N. Kourgiyas · G. P. Karatzas
School of Environmental Engineering, Technical University of
Crete, Chania, Greece
e-mail: zoi.dokou@enveng.tuc.gr

occurs in many coastal aquifers and can jeopardize groundwater quality if not detected in time (Dokou and Karatzas 2012). The adverse effects of seawater intrusion in productive aquifers involve the reduction in the available freshwater storage volume and the simultaneous contamination of production wells, given that less than 1 % of seawater is capable of rendering freshwater unsuitable for drinking and irrigation purposes (Werner et al. 2013). Groundwater contamination by nitrates is a problem related mainly to the spreading of organic and chemical fertilizers by farmers and, to some extent, to effluents from domestic sewage systems (Psarropoulou and Karatzas 2014). Nitrate (NO_3^-) contamination in groundwater is attributed to various non-point sources including fertilizer application, use of animal manure, septic tanks, and geological origins. The amount of NO_3^- that leach from agricultural areas into the groundwater depends on various natural factors such as soil type and climatic conditions (Mikkelsen 1992). In addition, shallow aquifers are more vulnerable to NO_3^- pollution as compared to deep or confined aquifers; however, surface or near-surface outcrops of confined aquifers can allow deeper downward migration of NO_3^- contamination (Daskalaki and Voudouris 2008). Sulfate (SO_4^{2-}) contamination is also common in Greece and is attributed to dissolution of sulfate minerals (gypsum and anhydrite) commonly found in the Quaternary aquifer matrices while anthropogenic sources include mining activities, fertilizer application, and industrial wastes.

Heavy metal contamination constitutes another major problem in various areas in Greece, receiving particular concern because of their strong toxicity even at low concentrations. Heavy metals are usually produced in mining areas and industrial zones but they can also be a product of geological weathering. The most important heavy metals examined here for the region of Greece are chromium (Cr), lead (Pb), and arsenic (As). The extensive use of Cr in industrial activities in combination to the geogenic origin of Cr from the leaching of ophiolitic rocks has resulted in multiple contaminated sites in Greece. The high toxicity and mobility of the hexavalent oxidation state of Cr (Cr(VI)) has increased the concern of scientists, grassroot organizations, and the public, pressuring for the establishment of a parametric value specifically for Cr(VI). Currently, the parametric value of 50 $\mu\text{g/L}$ for total Cr is being used in practice for Cr(VI). Pb contamination in groundwater originates from the dissolution of Pb from soil or anthropogenic sources such as mining and smelting, use of

sewage sludge as a soil conditioner, Pb arsenate pesticides and leaded gasoline. Pb has a limited mobility in groundwater and usually migrates sorbed onto colloidal-sized metal hydroxides. As is usually concentrated in sulfide-bearing mineral deposits, especially those associated with gold mineralization. It is relatively soluble in groundwater compared to other heavy metals depending on the pH, redox conditions, temperature, and solution composition. Man-made sources of As include mineral extraction, industrial activities, waste processing, and pesticides (Smedley and Kinniburgh 2002).

The need to avoid further deterioration of water quality and quantity in Greek aquifers has attracted a great deal of attention from governmental and regulatory bodies. Currently, they are seeking actions and examining possible remediation methods to ensure sustainable management and protection of water resources. In order to design successful remediation strategies and protect public health, it is very important to identify those areas that are most vulnerable to groundwater contamination and analyze the temporal and spatial distribution of contamination. Geostatistics offer an effective way to estimate (i) contaminant concentrations in un-sampled areas using variants of kriging (D'Acqui et al. 2007; Varouchakis et al. 2012; Venteris et al. 2014; Kourgialas and Karatzas 2015) and (ii) the probability that their concentration will exceed a pre-specified threshold using indicator kriging (Lu et al. 2007).

In a previous work, Daskalaki and Voudouris (2008) performed a synoptic review of the hydrochemical conditions of the porous aquifers in Greece, using collected groundwater quality data for Greece from 1998 to 2001. As an extension of this work, a more recent, extensive contamination database from monitoring wells that cover the entire Greek territory during the last decade (2000–2008) was used here in order to evaluate groundwater quality in Greece. Based on these records, the temporal and spatial distribution of groundwater contamination was studied for Cl^- , NO_3^- , and SO_4^{2-} as well as the most commonly encountered heavy metals (Cr, Pb, and As). Spatial and temporal patterns and trends in the occurrence of groundwater contamination were also identified highlighting the regions where the higher groundwater contamination rates have been detected across the country. Moreover, the seasonal distribution of the pollutants was investigated for the entire country. Then, based on the above maps, representative contaminated aquifers (Malia, Korinthiakos, and Asopos) were selected in order to analyze their water quality in more

detail. To this end, geostatistical techniques (various types of kriging and co-kriging) were used for the generation of groundwater quality maps in each aquifer and their performances were compared. In addition, indicator kriging was employed in order to map the probability of exceeding critical thresholds (set as the parametric values of the contaminant of interest in each case). The resulting groundwater contamination maps could be used in turn as a useful tool for water policy makers and water managers in order to assess remediation alternatives and develop successful management strategies.

Study areas

Greece

The country of Greece is located in the southeast Europe, covers an area of 132,000 km², and has a population that reaches 11,000,000 inhabitants. It has the longest coastline in Europe, exceeding 15,000 km along the Mediterranean Sea and much of its area is mountainous. The main aquifers in Greece are either karstic aquifers (carbonate rocks) or porous (alluvial and neogene deposits). Karstic aquifers cover more than 35 % of the Greek mainland and many of them are cropping out at the coast (Daskalaki and Voudouris 2008).

According to water resources legislation (1739/87 for the management of water resources), Greece is divided in 14 water districts: (1) West Peloponnese, (2) North Peloponnese, (3) East Peloponnese, (4) West Central Greece, (5) Epirus, (6) Attiki, (7) East Central Greece, (8) Thessaly, (9) West Macedonia, (10) Central Macedonia, (11) East Macedonia, (12) Thrace, (13) Crete, and (14) Aegean Islands that are presented geographically in Fig. 1. This division will be followed in this paper as well, in order to describe the temporal and spatial quality of groundwater in Greece. In the same figure, the locations of three selected areas (Asopos river basin in East Central Greece, Korinthiakos in North Peloponnese, and Malia in Crete) that will be further studied in more detail as presented.

Malia aquifer—seawater intrusion

The coastal aquifer under study, where the seawater intrusion phenomenon is very intense, is located near

the town of Malia, in Northern Crete, 40 km east of the city of Heraklion. The study area of 13 km² is characterized by a gentle slope to the north of the town of Malia and by mountains to the south. Sclerophyllous vegetation and complex cultivation patterns cover most of the study area. Other land uses include olive groves, natural grassland, non-irrigated arable land, and a small area of discontinued urban fabric around the towns of Malia and Mohos. The coastal karstic aquifer of Malia is developed in limestones of the Tripolis zone. Under these rocks, a series of alternating chloritic schistes, phyllites, and quartzites belonging to the Phyllite-Quartzite zone acts as the impermeable substrate of the extended region (Kallergis et al. 2000). The Tripolis series consists of faulted and karstified limestones, dolomites, and calcareous dolomites (Jurassic-Cretaceous and Triassic-Jurassic). The stratigraphy includes Neogene deposits that consist of bioclastic Messinian limestones and Quaternary clastic sediments. Along the coast, alluvial deposits and beach sand deposits are found. The first study of seawater intrusion of the local aquifer was performed by Lambrakis (1998) using hydrogeological and hydrochemical methods. They estimated an area of increased risk from seawater intrusion, based on the classification and interpretation of the hydrochemistry of groundwater using a Durov diagram. During recent years, over-pumping of the aquifer of Malia in combination with reduced rainfall has intensified the phenomenon of seawater intrusion (Lambrakis and Kallergis 2001). In addition, the existence of fractures perpendicular to the coast enables saltwater to travel long distances inland. The seawater intrusion phenomenon in this aquifer has been studied using numerical modeling and optimization tools by Karatzas and Dokou (2015) in order to provide alternative water management scenarios that will ameliorate the deterioration of the aquifer's water quality.

Korinthiakos—nitrate contamination

The coastal aquifer of Korinthiakos, located in North Peloponnese, is situated between the towns of Kiato and Lechaio and covers an area of about 55 km². It is bounded by a fault zone along the Athens–Patras national road to the South and by the Corinthian Gulf to the North. The primary use

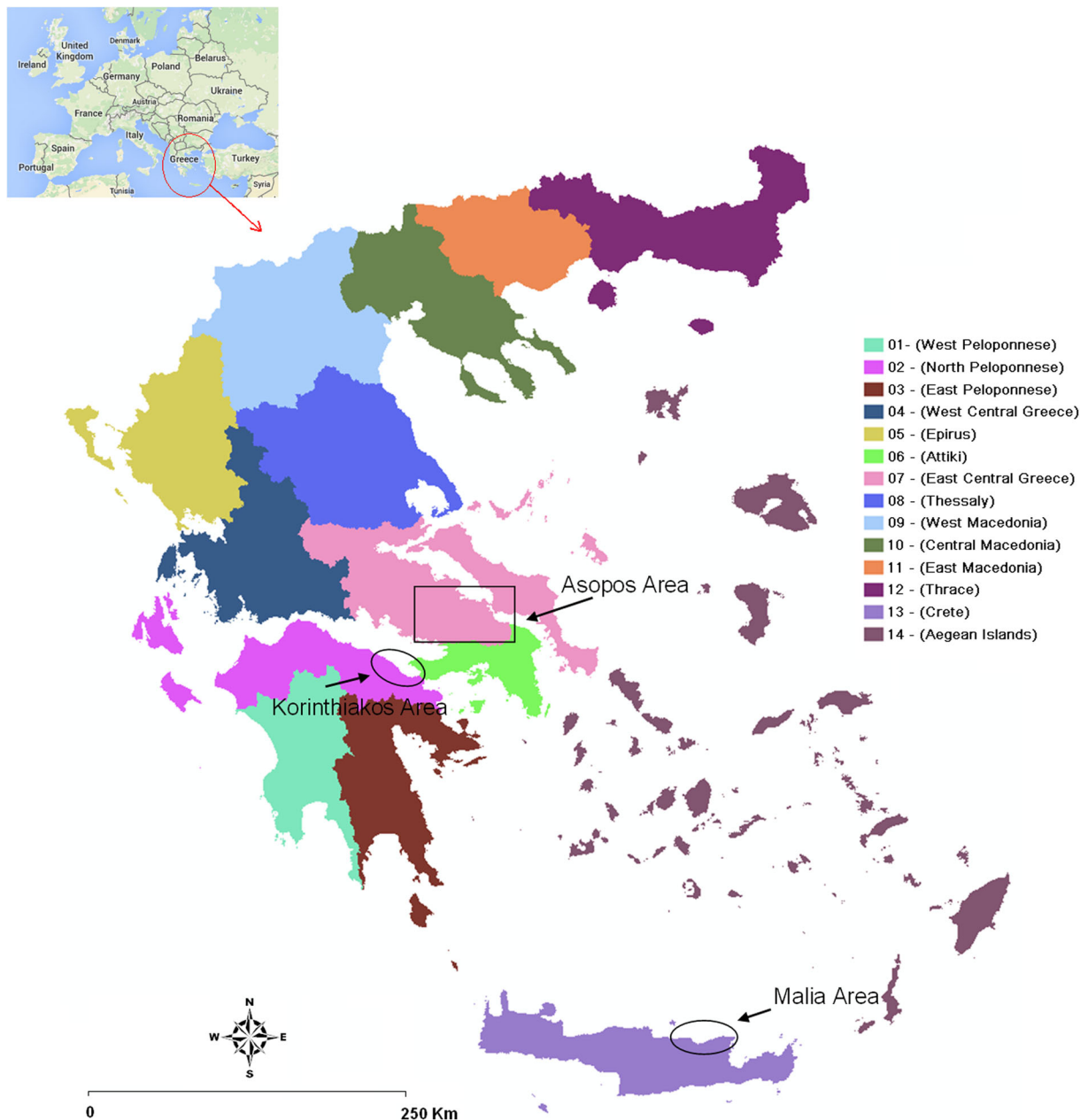


Fig. 1 Water districts of Greece and selected aquifers (Asopos, Korinthiakos, and Malia aquifers)

of the plain area is agricultural, while near the coast, residential areas have been expanding steadily over the years. The growing population and expanding irrigated land has resulted in over-pumping, excessive fertilization, and poorly treated wastewater disposal, rendering the aquifer vulnerable to water quantity and quality problems (Psarropoulou and Karatzas 2014) with NO_3^- contamination being the most prominent.

Asopos river basin—Cr(VI) contamination

The extended Asopos river basin that is studied here has an area of approximately 2900 km². The industrial sector bloomed during the last decades, due to the establishment of an industrial park during the late 1970s and early 1980s in the area of Inofyta that comprised of more than 450 industrial units. This growth resulted in the significant deterioration of water quality

of the water bodies (surface and groundwater) in the area. The most important issue in the area is related to the high concentrations of Cr(VI) that has been found to have both anthropogenic and geogenic origin (Moraetis et al. 2012; Panagiotakis et al. 2014; Dokou et al. 2015). The main geological formations encountered in the Asopos river basin are limestones, neogenic deposits, quaternary deposits, and ultrabasic rocks. Several locations with ultrabasic rocks, the main formation responsible for the geogenic origin of Cr(VI), have been observed in the greater area, especially in the eastern part of the Asopos river basin.

Materials and methods

Groundwater quality database

An extensive contamination database of monitoring wells that cover the entire Greek territory during the last decade was used in order to study the temporal and spatial distribution of various contaminants. This database is maintained by the Institute of Geology and Mineral Exploration (IGME) that has established a national network of more than 9300 wells for monitoring qualitative and quantitative properties of groundwater systematically (about once a month) for the 14 water districts. This work utilizes the quality information for the major ions (NO_3^- , SO_4^{2-} , and Cl^-) and selected heavy metals (Cr, Pb, and As). This database was enriched with contamination and water level data collected either by the Geoenvironmental Engineering Laboratory of the Technical University of Crete or obtained from various reports at the areas of interest: Cl^- concentrations (38 samples) and hydraulic head data (69 samples) for the years 1995–2010 for Malia aquifer (Paritsis 2001) and Kallergis et al. 2000), average NO_3^- concentrations (dry period 54 samples and wet period 45 samples) and depth to water table data (41 samples for dry and wet periods) for the years 1998–2007 for Korinthiakos aquifer (Psarropoulou and Karatzas 2014), and Cr(VI) concentrations (211 samples) and depth to water table data (593 samples) for the years 1995–2013 for the Asopos river basin (Dokou et al. 2015).

Statistical analysis

A statistical analysis of the available measurements for the major ions (NO_3^- , SO_4^{2-} , and Cl^-) and selected

heavy metals (Cr, Pb, and As) for the entire country was conducted in order to detect the spatial and temporal patterns and trends in groundwater quality. The average values were calculated for each water district for the entire monitoring period (2000–2008) in order to show the contamination spatial trend. In order to present the temporal trend for the entire country, the minimum, maximum, and average values were calculated yearly.

Statistical analysis was also performed for the contamination data of each of the three selected aquifers of interest (mean, max, min, and standard deviation). The distribution of each variable was also inspected for normality (skewness and kurtosis) and a suitable transformation (either Box-Cox or normal score) was performed in each case. Trend analysis was also performed in order to assess the need for trend removal before applying the kriging methods.

Geostatistical analysis

In this study, the spatial groundwater contamination risk for anionic elements and heavy metals was investigated for Greece for the time period 2000–2008. This process is performed in a geographic information system (GIS) environment where thematic maps are produced for every element. Raster maps of groundwater contamination in Greece for each of the anionic elements NO_3^- , SO_4^{2-} , and Cl^- and the cationic trace elements (heavy metals) Cr, Pb, and As were produced. Specifically, based on dense groundwater contamination data, for the entire country of Greece, and using the kriging interpolation method in GIS, an average groundwater contamination map for the time period 2000–2008 was created.

Several kinds of kriging and co-kriging (ordinary, simple, disjunctive) were utilized and their performances were compared in order to define the most accurate spatial distribution of NO_3^- in Korinthiakos, Cl^- in Malia, and Cr(VI) in the extended Asopos river basin. In addition, indicator co-kriging was applied in order to define the probability that the concentration of each contaminant of interest will exceed a pre-specified threshold. This threshold was set to the parametric value of each contaminant. All geostatistical modeling was conducted using the Geostatistical Analyst tool in ArcGIS environment.

Kriging methods are specifically designed to model spatial variability. One of their main advantages is that they not only provide an estimate of the value of

spatially distributed variables but also an assessment of the probable error associated with these estimates (D'Acqui et al. 2007). Kriging methods require a function that describes the spatial correlation structure of the variables of interest. Two functions commonly used for this purpose are the semivariogram (or simply called the variogram) and the covariance and are estimated from the available data (Rouhani and Mayers 1990). The variogram analysis consists of the experimental variogram (calculated from the data) and the variogram model (fitted to the data).

In order to calculate the experimental variogram the following formula is used (Isaaks and Srivastava 1989):

$$\gamma(h) = \frac{1}{2N(h)} \sum_{(i,j)_{h_{ij}=h}} (v_i - v_j)^2 \quad (1)$$

where h is the separation distance (lag), N is the number of pairs in a lag, and v_i and v_j are the data values at points i and j . Note that the summation is over only the $N(h)$ pairs whose locations are separated by h .

In most cases, it is expected that there will be a minimum variance at almost zero spacing (nugget) attributed to measurement errors or micro-scale variations created when measurements taken at very small distances are different (due to small-scale geologic variability, for example). The variogram usually levels out at some maximum value representing the amount of variation in the process that is assumed to generate data (sill) for separation distances larger than a certain value (range). Beyond this distance (range), the data are assumed to have no statistical dependence. Between zero spacing and the range, there are several different models to describe how the variogram changes. The most common model variograms used for this purpose are the spherical, Gaussian, exponential, hole effect, and K-Bessel variograms. In general, once a suitable variogram model is selected, it is then used to determine the kriging (distance) weights that are applied to the concentration data located within a prespecified search radius, in order to provide concentration estimates at unsampled locations and create a concentration map. This procedure varies depending on the type of kriging method used.

In this work, experimental variograms were calculated from the data and model spherical variograms were fitted in all cases. For each data set, an iterative procedure was used where a lag size was incrementally adjusted and then tested by cross validation in order to determine the best fit. An initial lag size was set to the

average distances between samples, as suggested by Isaaks and Srivastava (1989). Then, the nugget was adjusted manually, in order to provide a better fit. The points for each kriging estimate were chosen using a circular search scheme, with 10 neighbors used for each estimate. The final model variogram was chosen on the basis of the lowest RMSE from cross validation. Representative variograms for each test case, showing the spatial dependence of data, are presented in Fig. S1 (supplementary material) only for one of the kriging methods (OK) for brevity reasons. It is observed that moving from a small-scale (Malia) to a medium-scale (Korinthiakos) and finally to a large-scale study area (Asopos), the lag size and range increases accordingly. The largest variability is found in the datasets of Cl^- (Malia) and NO_3 (Korinthiakos), while for the Asopos data, less variability is encountered, due to the fact that a large number of very low concentrations (and non-detect values that were set to the detection limit of $5 \mu\text{g/L}$) are included in the dataset.

Ordinary kriging

Ordinary kriging (OK) is a linear interpolator that estimates a value at a point of a region for which the variogram is known, without prior knowledge about the mean of the distribution. In OK, a random function model is used, in which the bias and error variance can both be calculated and then weights are chosen for the nearby samples such that they ensure that the average error for the model is zero and the modeled variance is minimized. In OK, in order for the estimator to be unbiased, the sum of these weights needs to equal one (Isaaks And Srivastava 1989). The estimation equation is a linear weighted combination of the form:

$$\hat{v}_0 = \sum_{k=1}^n w_k \cdot v_k, \text{ With The Constraint Of } \sum_{k=1}^n w_k = 1 \quad (2)$$

where

- \hat{v}_0 Is the desired estimate at point 0
- w_k Are the weights at each neighboring sampling point K and
- v_k Are the available measurements at each neighboring sampling point K .

Simple kriging

Simple kriging (SK) is also a (weighted average) linear estimator, similar to OK, with the difference that prior knowledge of the mean is required. The mean of the available measurements is used in the estimation leading to a smoother estimation map. The requirement of the sum of weights to equal unity does not apply to SK.

Disjunctive kriging

Disjunctive kriging (DK) is a form of nonlinear kriging (i.e., a nonlinear estimator) which on one hand offers an improvement over linear kriging methods and on the other it does not require the knowledge of the $n+1$ joint probability distributions necessary for similar estimation methods. It was first proposed by Matheron (1976) as a simplified alternative of conditional expectation which only requires that the bivariate distributions of the $n+1$ variables are known (Yates et al. 1986). The calculations necessary to make an estimate are basically the same as for simple kriging only performed k times per estimate and Hermite polynomials of order k are utilized for this purpose.

Co-kriging

Co-kriging offers a way to improve the prediction of a variable (primary) by incorporating information of secondary variables that exhibit some correlation with the primary variable. The usefulness of the secondary variable is highlighted especially in cases where the primary variable is undersampled, as is the case for the Malia and Asopos areas; for the Korinthiakos aquifer, the number of primary and secondary sampling points is roughly the same. In this work, the estimation of the primary variable of concentration was enhanced by including depth to water table measurements for the cases of NO_3^- contamination in Korinthiakos and Cr(VI) pollution in Asopos (for which the depth of the vadose zone plays a significant role for the leaching process). Specifically, the depth to water table (unsaturated zone depth) is analogous to the time needed for contaminants to reach the unconfined aquifer. The shallower the depth, the greater is the risk to the aquifer (Prasad et al. 2011). For the case of Cl^- contamination, the variable of hydraulic head was

used because, according to Ghyben-Herzberg relation, the seawater intrusion problem is directly related to the freshwater hydraulic head maintained in the coastal aquifer. The higher the freshwater hydraulic head, the smaller the intrusion of seawater inland (Werner et al. 2013). Co-kriging was performed for all types of kriging (ordinary, simple, and disjunctive) in order to find the best estimator (Isaaks and Srivastava 1989).

Indicator kriging

The goal of indicator kriging (IK) is different for other types of kriging. It is used to estimate the probability of exceeding some user defined threshold value, by transforming the data into binary variables. The main advantage of indicator kriging is that it is non-parametric; thus, no assumption about the variable distribution is required; and the experimental CDF is used instead, by dividing it into sample quantiles. Simple kriging (or co-kriging) is used at each quantile in order to provide the estimates. Indicator kriging is very useful for the development of contaminant concentration maps in cases where the identification of areas of high concentrations exceeding the parametric values for drinking water or other uses is of interest. For the areas with lower concentrations the knowledge of the exact concentration values is not as important, as long as they remain below the parametric value.

Cross-validation and prediction errors

Cross-validation (CV) was used to compare the performance of each kriging technique (OK, SK, DK, co-OK, co-SK, co-DK, and IK) using various variogram types. Cross-validation was performed by eliminating sequentially each data point from the data set and then estimating it using the constructed model. Various statistical measures were calculated in order to compare the goodness of fit of each model: (1) the mean error (ME), (2) the root mean square error (RMSE), (3) the average standard error (this prediction error comes from the kriging equations), (4) the standardized error of the mean (SEM), and (5) the standardized root mean square error (SRMSE). For an accurate model, the ideal values for the above error measures are the following: (1) zero, (2) as small as possible, (3) as small as possible, (4) zero, and (5) one, respectively.

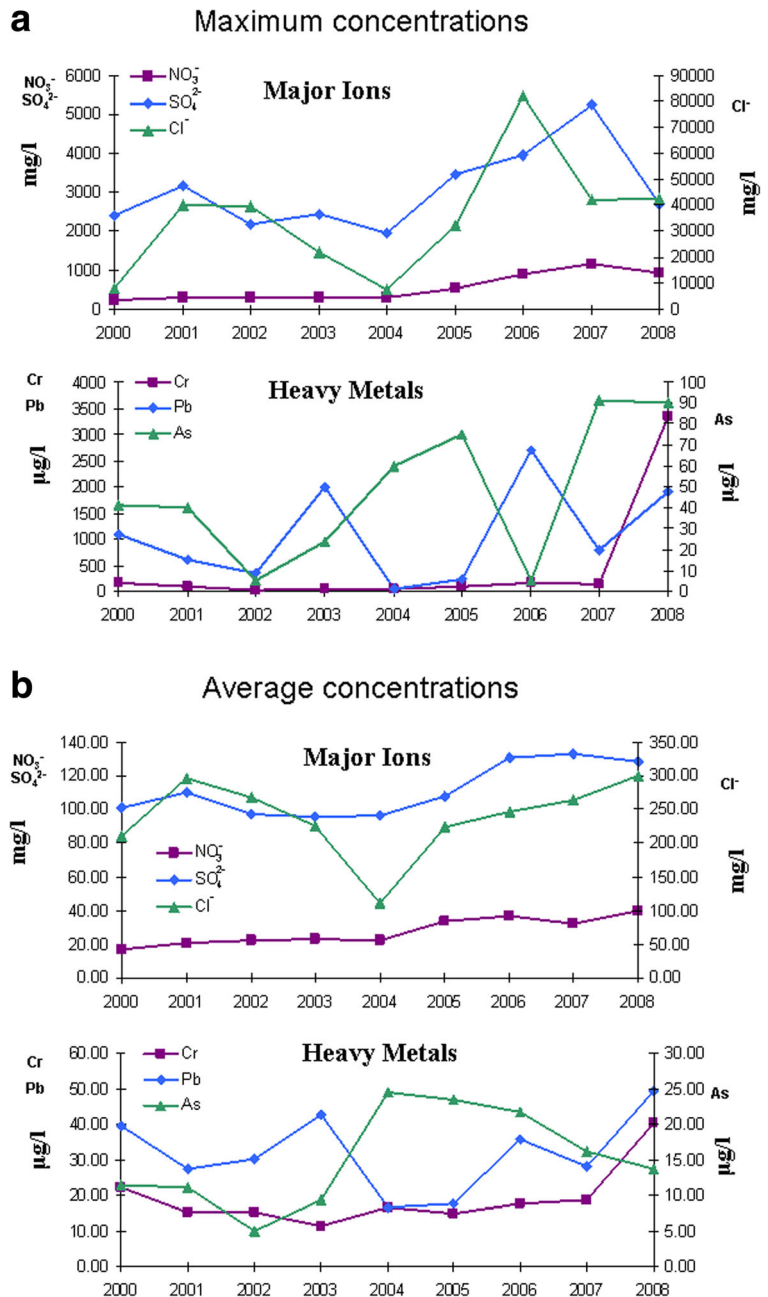
Results and discussion

Temporal analysis of countrywide data

For the temporal analysis of the contamination data from the IGME database, the maximum (Fig. 2a) and average values (Fig. 2b) for the entire Greek territory were calculated for each year of the monitoring period (2000–2008). The temporal distributions of NO_3^- and

SO_4^{2-} concentrations follow a similar pattern with an increasing trend over the years. The average concentrations for both these ions are kept below the parametric value (50 and 250 mg/L, respectively) although the corresponding maximum values (1153 mg/L for NO_3^- and 5240 mg/L for SO_4^{2-}) are both observed in 2007 in the districts of Eastern and Western Peloponnese, respectively. Regarding Cl^- contamination that is often an indication of seawater intrusion, the average values

Fig. 2 Temporal analysis of the **a** maximum and **b** average concentration values of the major ions and heavy metals for the entire Greek territory (statistical analysis performed on raw data from the IGME database)



are just above the parametric value of 250 mg/L for the entire monitoring period except in 2004 when the average concentration falls at about 100 mg/L. The extremely high maximum values for Cl^- are indicative of anthropogenic contamination and cannot be attributed to seawater intrusion effects.

Among the heavy metals examined in this work, Pb shows the most elevated values that fluctuate temporally but are always above the parametric value of 10 $\mu\text{g/L}$. Values as high as 2700 $\mu\text{g/L}$ have been observed in Eastern Central Greece in 2006 that are considered highly toxic. Cr concentrations show an increasing trend over the years but their average values are kept below the parametric value of 50 $\mu\text{g/L}$. Values as high as 3000 $\mu\text{g/L}$ observed in 2008 are attributed to local burial of industrial wastes. As concentrations also show an increasing trend, and after 2003, their average values exceed the parametric value of 10 $\mu\text{g/L}$, which is an alarming phenomenon. Values as high as 90 $\mu\text{g/L}$ have been observed in the Aegean island water district in 2007. In general, although the average values for the year 2007 are not very elevated for most of the contaminants examined here, the maximum values for NO_3^- , SO_4^{2-} , and As have all been observed in that year. This could be related to the fact that 2007 was recorded as one of the driest years in Greece during the period of 2000–2008 (Founda and Giannakopoulos 2009). It is common for concentration contamination levels to increase in dry conditions, because the contaminants are dissolved in smaller volumes of water.

Spatial analysis of countrywide data

For the spatial analysis of groundwater contamination from the major ions and heavy metals, firstly, a bar graph (Fig. 3) was generated that shows the average concentration values for Cl^- , NO_3^- , and SO_4^{2-} and the selected heavy metals (Cr, Pb, and As). The conclusions that can be drawn from this figure are that the seawater intrusion phenomenon is a major problem with very high Cl^- concentrations that are more pronounced in the regions of Attica and Thrace, while on average, NO_3^- and SO_4^{2-} concentrations are not as significant. For the heavy metal, concentrations on average Cr(VI) show low levels of concentration that are below the corresponding parametric value for drinking water. For Pb, the average concentration values are all above the parametric value except for Epirus and Central Macedonia where they are close to the regulatory limit. This shows

that Pb contamination poses a significant threat to the groundwater reserves in the majority of the Greek aquifers, suggesting the need for immediate remediation measures nationwide. As concentrations are a little above the regulatory limit for some regions including East Central Greece, Central Macedonia, Crete, and the Aegean islands. Note that for As, there were no available measurements for the water district of Epirus.

The geostatistical technique of kriging was also used in order to generate groundwater concentration maps (Fig. 4) for the contaminants of interest, including five classifications in each map. The light blue colors correspond to concentration values below and the yellow color to values just below the parametric values of each contaminant. The dark orange and red colors depict concentrations that exceed the regulatory limits.

Based on the results for the major ions, very high SO_4^{2-} concentrations are limited in the regions of Heraklion and Lasithi in the water district of Crete, in the island of Corfu (Epirus) and in the water district of Central Greece. At the rest of the areas, the SO_4^{2-} concentrations are in low levels. Regarding the spatial distribution of NO_3^- , it is concentrated in the areas of Attica, Central Macedonia, Thessaly and North and East Peloponnese. Thessaly and Korinthiakos (in North Peloponnese) are primarily agricultural regions that are particularly vulnerable to nitrate pollution caused by the overfertilization of crops. From the contamination maps it is confirmed that seawater intrusion is a major problem in Greece; almost the entire coastline is affected in various degrees except from parts of the coast of South Crete, North Evia, and West Macedonia. This can have significant implications for the future of groundwater reserves because of the large extent of the country's coastline. Overexploitation of coastal aquifers induces the phenomenon, especially in karstified aquifers that are very common in Greece and are in greater risk because of the existence of irregular fissures and solution openings that enable seawater to enter the aquifer and travel further distances towards the mainland.

Regarding heavy metal contamination, high As concentrations are located in the East Chania Prefecture and Lasithi (water district of Crete) and in Chalkidiki (water district of Central Macedonia), where the gold mines are located; hence, significant leaching of heavy metals occurs in the groundwater. Cr concentrations are not very high in most Greek regions with the exception of (i) Chalkidiki, due to the same reason mentioned above, and (ii) Thiva, where the Asopos river basin is located

Fig. 3 Average concentration values of the major ions and heavy metals for each water district

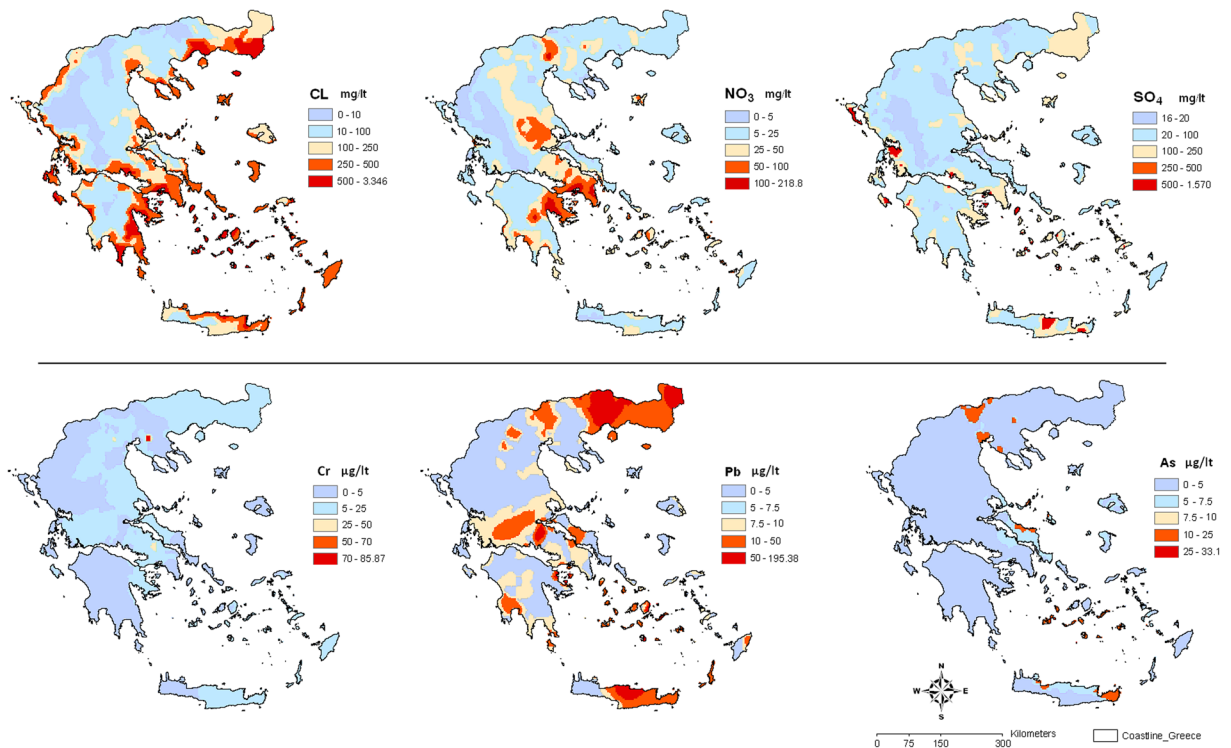
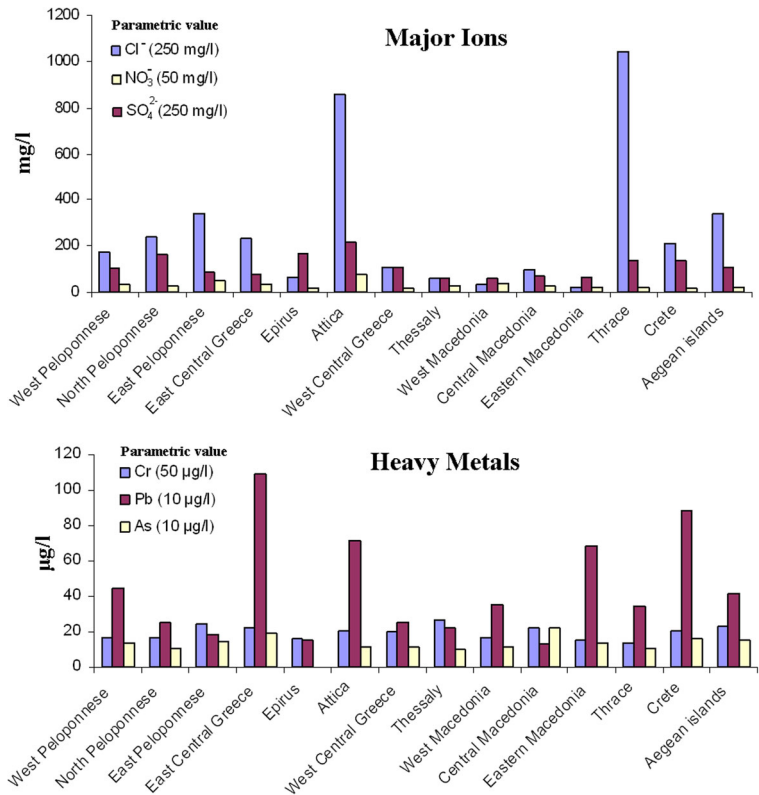


Fig. 4 Spatial distribution of average ion and heavy metal concentrations for the country of Greece

which is a unique case of both anthropogenic (industrial) and geogenic origin of Cr contamination (Moraetis et al. 2012). Pb is found in very high concentrations in many regions of Greece such as Central and East Crete, Thrace, Central and East Macedonia, West and Central Greece, West Peloponnese, and some of the Aegean islands. This supports the conclusion mentioned above, i.e., that Pb contamination appears to be a serious problem for the country of Greece.

Spatial analysis of three selected aquifers

The statistics of the contaminant concentration datasets of the three case studies are presented in Table S1 (supplementary material). Table S2, also in supplementary material, presents measures of the error of the estimation for all kriging methods performed (OK, SK, DK, and their co-kriging counterparts as well as indicator co-kriging) for all three case studies. Various indicators are calculated, as choosing only one of them in order to judge a model's performance might lead to biased results. Nevertheless, the most representative measures are the ones that have been standardized (mean error standardized and RMSE standardized) to remove the dependence on the units in which the variable is measured.

Malia area

For the Malia aquifer, Cl^- concentration data were available for 38 wells. A maximum value of 812 mg/L was observed, which is well over the parametric value of 250 mg/L for drinking water, indicative of the severe seawater intrusion problem in the area. The mean value of the dataset (277.75 mg/L) is slightly above the parametric value as well, supporting the same notion. The data did not follow a normal distribution (skewness=1.12 and kurtosis=3.99); thus, a Box-Cox transformation was performed with a parameter $\lambda=0.48$, in order to ensure the normality condition for the OK and SK kriging and co-kriging methods. For DK and co-DK, an alternative option of using a normal score transformation, with three Gaussian kernels for this dataset, was available that produced better results (Table S1).

Among the kriging estimation methods that were used for mapping Cl^- concentration, the most accurate results were obtained when the hydraulic head dataset was included in the estimation (co-kriging) and specifically for the non-linear estimators of co-OK (best

RMSE standardized) and co-DK (best mean error standardized). For this case study, it is difficult to say which model performs better; it can be concluded that both estimators could be safely used, with acceptable accuracy (Table S2). For brevity reasons, only the resulting concentration map for co-DK is shown in Fig. 5a, along with the locations of the sampling wells and major faults in the area. From the figure, it is evident that in the center of the study area the Cl^- concentration values are relatively small when compared to those to the eastern and western parts. This is mainly due to the existence of faults along the eastern and western parts (represented by red lines in Fig. 5a), which acts as channels that can drive seawater intrusion asymmetrically inland rapidly and over long distances. This is also in agreement with the fact that hydraulic head levels are higher in the center and lower in the eastern and western parts of the study area. Therefore, the central area can be seen as a recharge zone and the other two areas as zones where fresh- and seawater mixing phenomena occur. The lowering of the water table levels, that enhances the seawater intrusion problem, has been a result of extensive pumping in the area for the past decades, increasing over the years due to a combination of population growth, increased touristic activities and decreasing precipitation during the summer months. The yellow line in Fig. 5a represents the contour of 1 % of seawater (250 mg/L Cl^- concentration) that is capable of rendering freshwater unsuitable for drinking purposes. The threshold of Cl^- concentration that causes damages to plants and crops appears to be cultivar dependent. The study area is dominated by olive trees, which are resilient in saline water and vegetable crops, which are more sensitive to high levels of salinity. Taking into account published information on the effects of salinity on growth and production, a suggested Cl^- concentration threshold is 1 dS/m (or 300 mg/L Cl^-) for vegetable crops (eggplants, tomato, cucumber, and onion) and 2.5 dS/m (or 800 mg/L Cl^-) for olive trees (Chartzoulakis 2005). Based on the above, the thresholds for drinking and irrigation of vegetable crops are very close; thus, only the lower of the two (250 mg/L) is shown in Fig. 5a and is used for the indicator kriging map in Fig. 5b, which presents the probability of Cl^- concentrations exceeding this parametric value. From this map, it is evident that in the eastern and western parts near the fractures, the probability of exceeding the parametric value is higher than that in the center of the region, as expected.

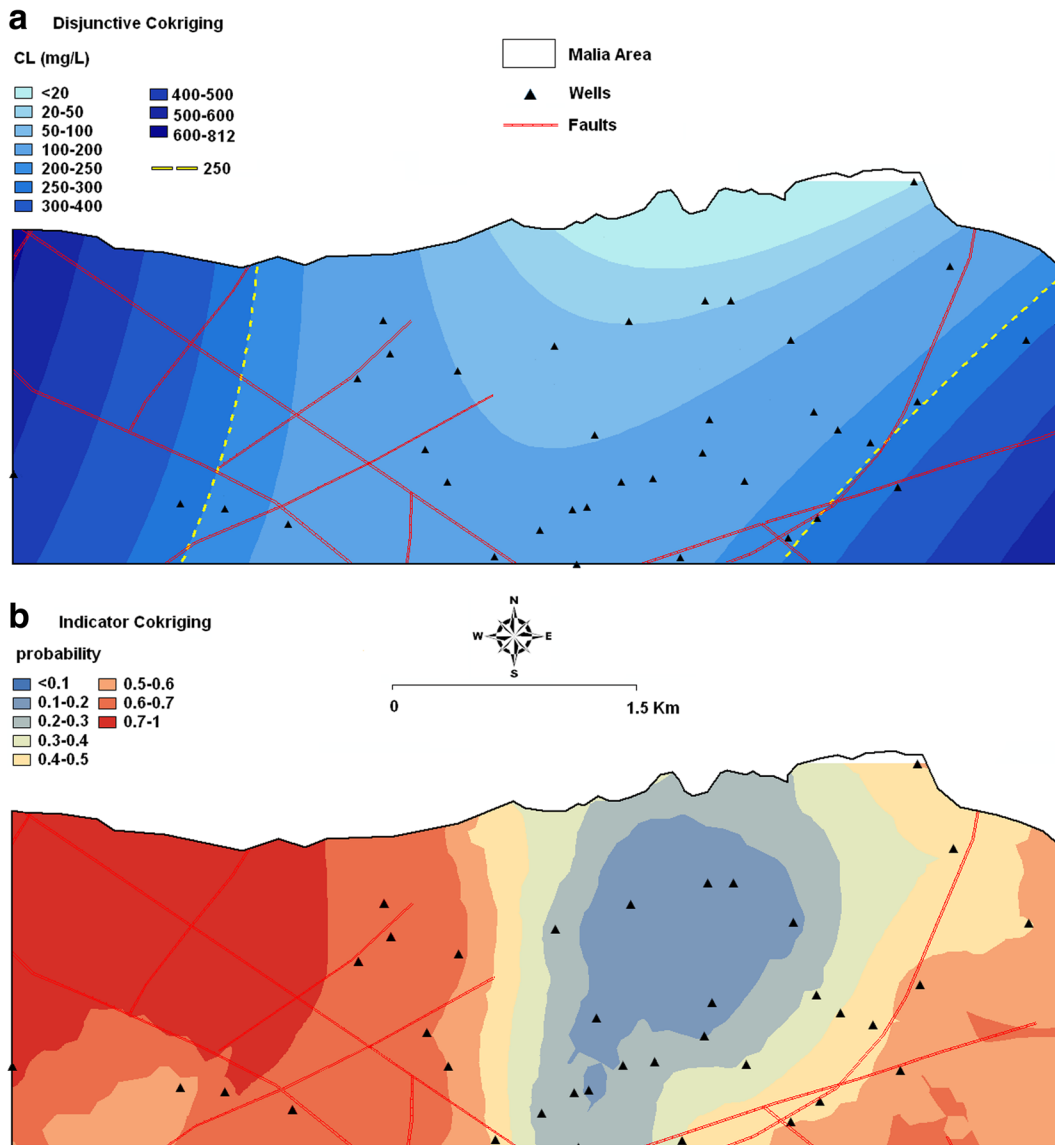


Fig. 5 **a** Disjunctive and **b** indicator co-kriging results for Malia aquifer

The Korinthiakos area

The available sampling data for the Korinthiakos aquifer were divided into dry (54 samples) and wet periods (45 samples), and the average concentrations in each point were obtained. Separate concentration maps were created for each period. The maximum (140.47 mg/L for the dry and 189.8 mg/L for the wet period) and mean values (140.47 mg/L for the dry and 189.8 mg/L for the wet period) were all over the parametric value of 50 mg/L, highlighting the NO_3^- pollution problem in the area, originating

mostly from the use of fertilizers. A transformation of the data was required in both cases since neither followed a normal distribution (dry period: skewness=0.71 and kurtosis=2.82; wet period: skewness=0.92 and kurtosis=4.16); thus, a Box-Cox transformation was performed with λ parameters of 0.6 (dry) and 0.65 (wet), in order to ensure normality (for OK and SK kriging and co-kriging methods). For DK and co-DK, normal score transformation with four Gaussian kernels for the dry dataset and five Gaussian kernels for the wet dataset was used with better results (Table S1).

Among the kriging estimation methods that were used for mapping NO_3^- concentration for the dry season, the most accurate results (both in terms of mean error standardized and RMSE standardized) were obtained with co-DK, using the depth to the water table dataset as a secondary variable (Table S2). The inclusion of depth measurements in the calculations (co-kriging) improved the results as there is a high correlation between this variable and NO_3^- pollution; the shallower the aquifer, the more vulnerable it is to NO_3^- pollution.

For the wet season, the mean error standardized is better for co-DK while RMSE standardized is better for DK. This result suggests that it is unclear if the use of the depth measurements increased the accuracy of the model in the wet season. This can be partly attributed to the fact that fertilizers are applied in the area during the wet months of January and February when, due to the increased rainfall, the leaching of NO_3^- and its percolation through the vadose zone is rapid, influenced mainly by the amount of infiltrated water and less than the depth of the vadose zone (as opposed to the dry season). Taking into account that the use of a secondary variable increases the complexity of the estimator, DK might be preferable to co-DK, based on the principle of parsimony. Nevertheless, the results for co-DK are shown for the wet period as well, for coherence reasons with the rest of the test cases and the dry period results (Figs. 6a and 7a).

A temporal variation of NO_3^- concentration is evident from the figures, with higher concentrations observed during the wet period. This is mainly due to the more intensive fertilizer application during the winter months. For both periods, the highest NO_3^- concentrations are observed in the eastern part of the Korinthiakos area. According to the land use information of the area, on the eastern part of the region, intensive complex cultivation systems exist, while in the rest of the region, mainly citrus orchards and vineyards are present. In complex cultivation systems, a common agricultural practice is the frequent fertilizer application combined with intensive irrigation all year round. This results in more elevated NO_3^- concentration in these areas, compared to the rest of the cultivated regions of the area.

The yellow line that represents the value of 50 mg/L has a similar shape on the eastern part of the region for the two periods, while on the western part of the region, the area that exceeds this limit is located mainly along the south border for the dry season; for the wet season, it reaches further north mainly in the middle part of the Korinthiakos plain.

Figures 6b and 7b show the indicator kriging results. The probability of exceeding the parametric value for NO_3^- is higher in the eastern part of the study area in both periods (wet and dry) with the high probabilities covering a larger area during the wet season.

The Asopos area

The available sampling data for the extended Asopos area included 211 Cr(VI) concentration samples. The maximum (156 $\mu\text{g/L}$) value of the data set was above the parametric value of 50 $\mu\text{g/L}$ for total Cr (a parametric value for Cr(VI) has yet to be established). The mean value (20.65 $\mu\text{g/L}$) is below this limit. The data were highly skewed (skewness=2.66 and kurtosis=11.54) requiring a transformation; for OK and SK kriging and co-kriging methods, a Box-Cox transformation was performed with $\lambda=0.1$ (very close to the log-normal distribution) and for DK and co-DK a normal score transformation with four Gaussian kernels was used (Table S1).

Among the kriging estimation methods that were used for mapping $Cr(VI)$ concentration, the most accurate results were obtained when the depth to water variable as secondary information for co-DK (Table S2). From Fig. 8a, it is observed that three major problematic zones (yellow areas) exist in the area, where Cr(VI) concentration levels reach 156 $\mu\text{g/L}$. These regions are mainly located in industrial zones, thus attributed to anthropogenic activities. From Fig. 8b that presents the indicator kriging results for the extended Asopos river basin area, it becomes apparent that in these regions the probability of exceeding the parametric value for total Cr is elevated. Given the high toxicity of Cr(VI), a significant risk for human health is posed in these areas. A general Cr(VI) background concentration resulting from the leaching of ophiolitic rocks can also be inferred from Fig. 8a, which could be set to about 20 $\mu\text{g/L}$. This should be taken into account for the future establishment of threshold and parametric values for Cr(VI) in the area and for the decision on the appropriate remediation efforts to be applied in order to ameliorate the contamination problem.

Conclusions

In this work, an evaluation of the groundwater quality in the main water districts of Greece was

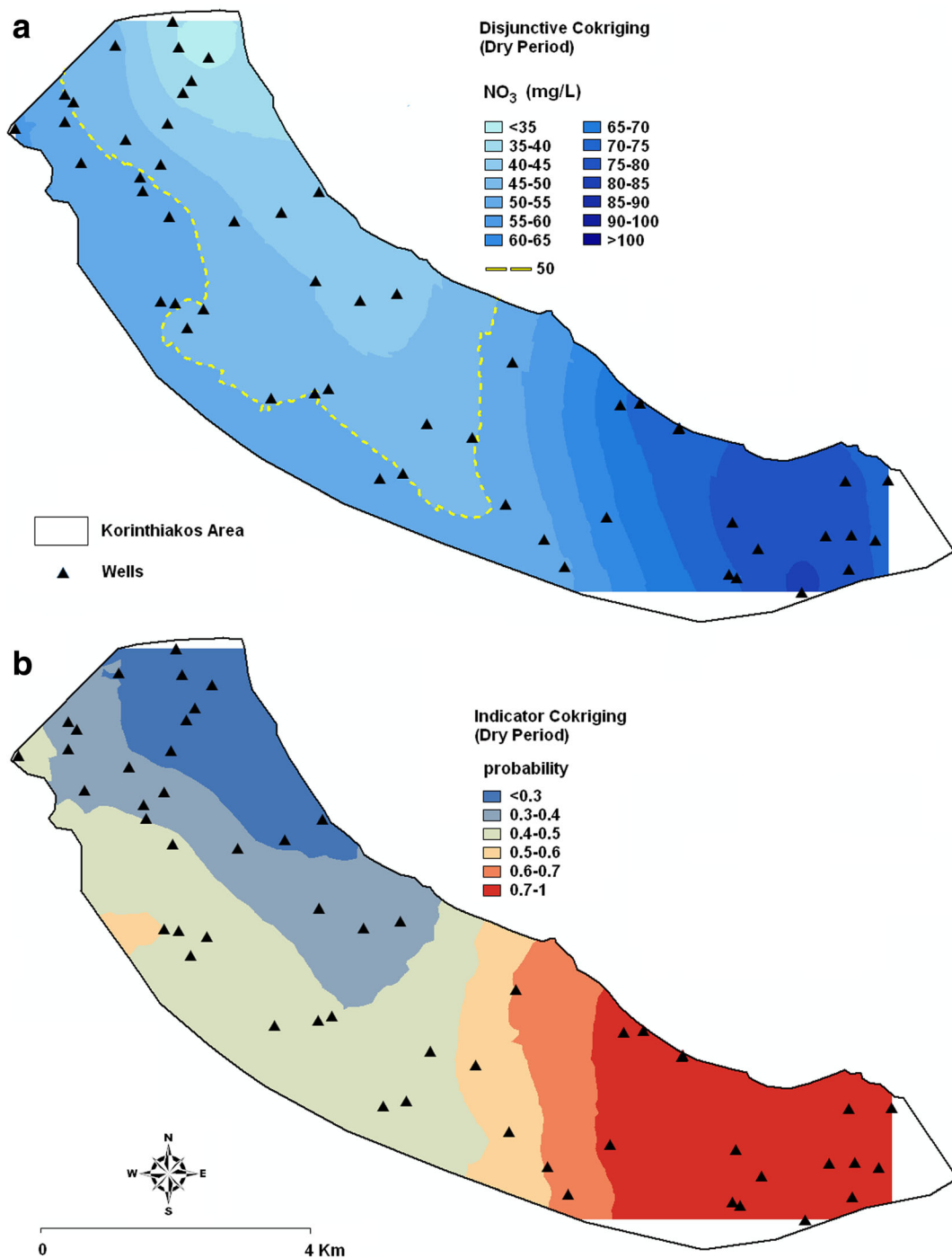


Fig. 6 a Disjunctive and b indicator co-kriging results for Korinthiakos aquifer for the dry period

performed in order to assess contamination risk. Based on the results, a major problem is seawater intrusion that is significant in almost the entire coastline of the country and particularly in the country's islands. Moreover, high NO_3^- concentrations are

observed in major agricultural areas such as Thessaly and Korinthiakos, due to the intense use of fertilizers and agrochemicals. Regarding heavy metal contamination, Pb is found in very high concentrations in many regions of Greece, i.e., Thrace and the

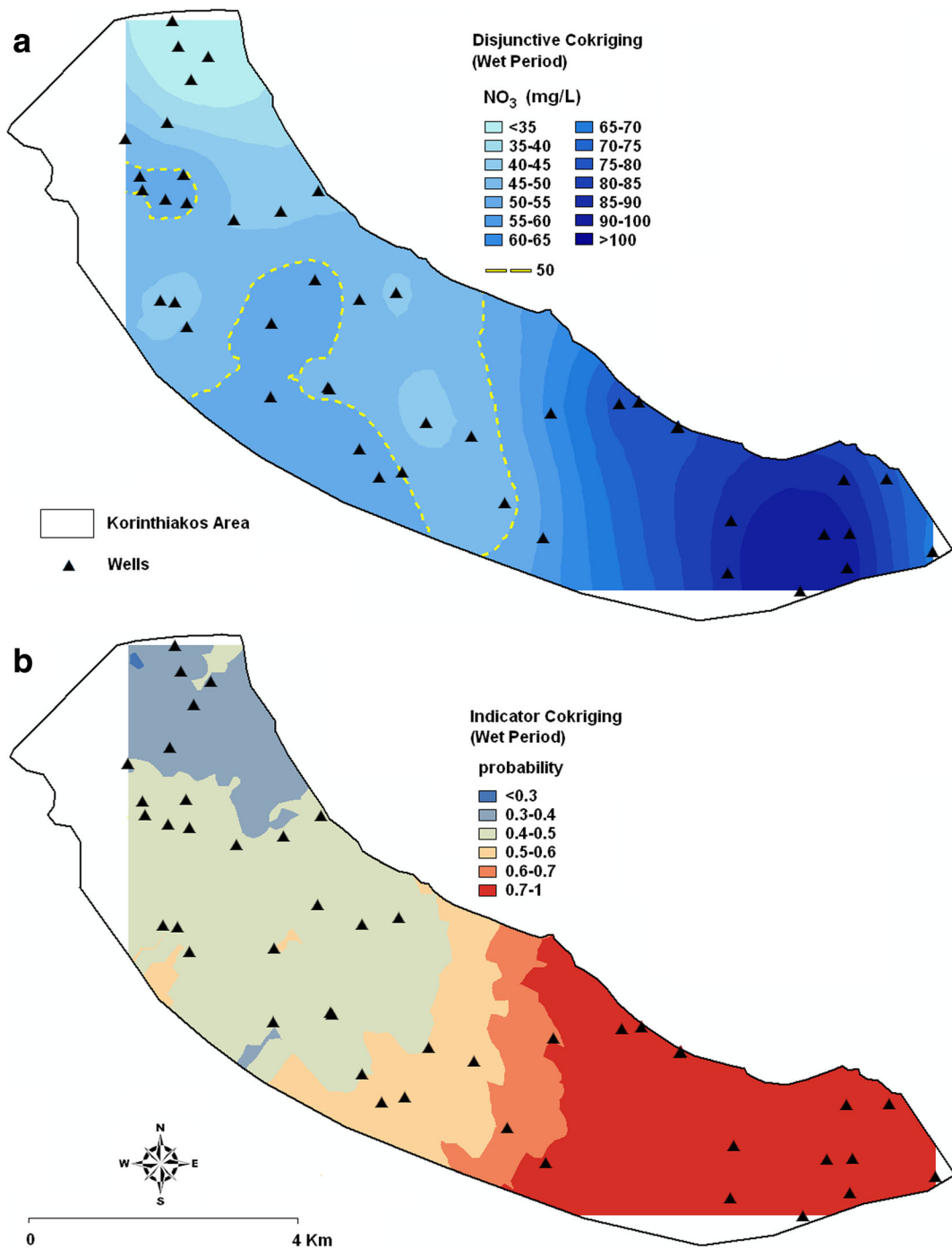


Fig. 7 a Disjunctive and b indicator co-kriging results for Korinthiakos aquifer for the wet period

central and eastern parts of Crete. As concentrations show an increasing trend after 2003 that is a local problem in specific areas of the water districts of Central Macedonia and Crete. The same conclusion is drawn for the Cr(VI) contamination that is also a

local phenomenon in the areas of Chalkidiki and the extended Asopos river basin.

Three aquifers (Malia, Korinthiakos, and Asopos) that present the most common contamination problems in Greece were analyzed in more detail using

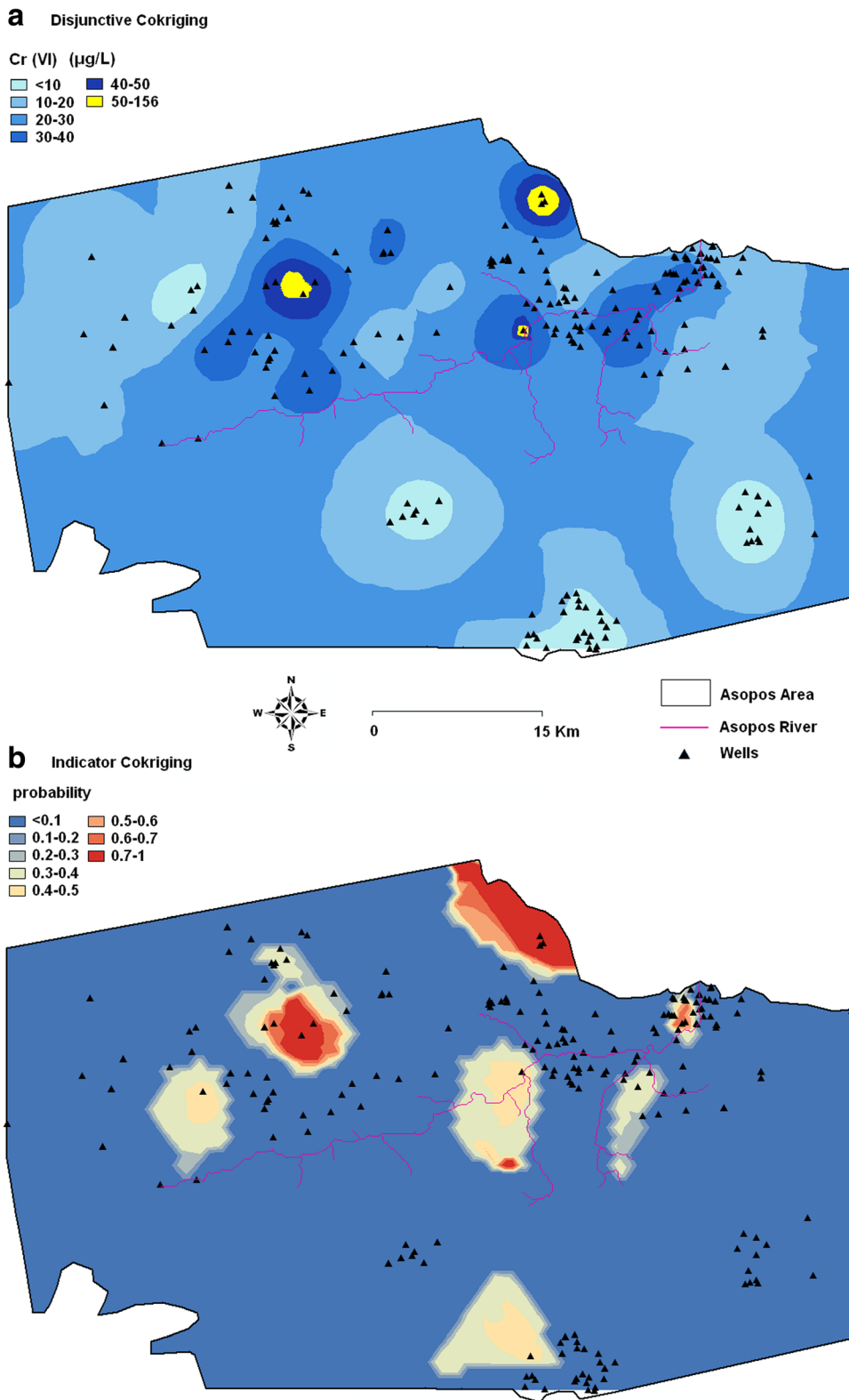


Fig. 8 a Disjunctive and b indicator co-kriging results for the extended area of Asopos river basin

geostatistical techniques (OK, SK, DK, and their co-kriging counterparts as well as indicator kriging). For the Korinthiakos area (dry season) and the Asopos extended area, the comparison of the standardized RMSE and standardized mean error indicators suggested that co-DK was the best estimator. For the Malia area, both co-OK and co-DK showed similar accuracy levels. For the wet season of Korinthiakos area, the mean error standardized is better for co-DK while RMSE standardized is better for DK. This result suggests that it is unclear if the secondary variable data used (depth to water level) increase the accuracy of the model in this case. This can be partly attributed to the fact that during the wet season, due to the increased rainfall, the leaching of NO_3^- and its percolation through the vadose zone is rapid, influenced mainly by the amount of infiltrated water and less than the depth of the vadose zone (as opposed to the dry season). Taking into account that the DK is the simpler model for the two, it might be preferable in this situation.

The contamination maps produced for the Malia aquifer showed that the Cl^- concentration values are smaller in the central part as opposed to the eastern and western parts, a fact attributed mainly to the existence of faults along the eastern and western parts that are able to transport saltwater rapidly and over long distances inland. At the Korinthiakos plain, a temporal and spatial variation of NO_3^- concentrations was observed with higher concentrations occurring during the wet period at the eastern part of the Korinthiakos area. At the extended Asopos river basin, the spatial patterns revealed three major problematic zones (yellow areas) with Cr(VI) concentration levels reaching 156 $\mu\text{g/L}$. These regions are mainly located in industrial zones, thus attributed to anthropogenic activities. Given the high toxicity of Cr(VI), a significant risk for human health is posed in these areas.

The results of this study could be used as a useful management tool for planning the appropriate actions in order to minimize groundwater risk and ensure the sustainability of water resources, based on the specific characteristics and problems of each water district.

Acknowledgments The authors would like to thank the Greek Institute of Geology and Mineral Exploration (IGME) for providing the contaminant monitoring database used in this work.

References

- Chartzoulakis, K. S. (2005). Salinity and olive: growth, salt tolerance, photosynthesis and yield. *Agricultural Water Management*, 78, 108–121.
- D'Acqui, L. P., Santi, C. A., & Maselli, F. (2007). Use of ecosystem information to improve soil organic carbon mapping of a Mediterranean island. *Journal of Environmental Quality*, 36, 262–271.
- Daskalaki, P., & Voudouris, Z. K. (2008). Groundwater quality of porous aquifers in Greece: a synoptic review. *Environmental Geology*, 54, 505–513.
- Dokou, Z., & Karatzas, G. P. (2012). Saltwater intrusion estimation in a karstified coastal system using density-dependent modelling and comparison with the sharp-interface approach. *Hydrological Sciences Journal*, 57(5), 985–999.
- Dokou, Z., Karagiorgi, V., Karatzas, G. P., Nikolaidis, N. P., & Kalogerakis, N. (2015). Large scale groundwater flow and hexavalent chromium transport modeling under current and future climatic conditions: the case of Asopos River Basin. *Environmental Science and Pollution Research*. doi: 10.1007/s11356-015-5771-1.
- Founda, D., & Giannakopoulos, C. (2009). The exceptionally hot summer of 2007 in Athens, Greece—a typical summer in the future climate? *Global and Planetary Change*, 67, 227–236.
- Isaaks, E. H., & Srivastava, R. M. (1989). *An introduction to applied geostatistics*. New York: Oxford University Press.
- Kallergis, G., Lambrakis, N., Voudouris, K., & Kokkalas, S. (2000). *Hydrogeological Investigation of the Municipality of Malia area*. Patras: University of Patras, Department of Geology.
- Karatzas G. P., & Dokou, Z. (2015). Managing the saltwater intrusion phenomenon in the coastal aquifer of Malia, Crete using multi-objective optimization. *Hydrogeology Journal*, 23(6), 1181–1194.
- Kourgialas, N. N., & Karatzas, G. P. (2015). An integrated approach for the assessment of groundwater contamination risk/vulnerability using analytical and numerical tools within a GIS framework. *Hydrological Sciences Journal*, 60(1), 111–132.
- Lambrakis, N. (1998). The impact of human activities in the Malia coastal area (Crete) on groundwater quality. *Environmental Geology*, 36(1–2), 87–92.
- Lambrakis, N., & Kallergis, G. (2001). Reaction of subsurface coastal aquifers to climate and land use changes in Greece: modeling of groundwater refreshing patterns under natural recharge conditions. *Journal of Hydrology*, 245, 19–31.
- Lu, P., Su, Y., Niu, Z., & Wu, J. (2007). Geostatistical analysis and risk assessment on soil total nitrogen and total soil phosphorus in the Dongting Lake Plain Area, China. *Journal of Environmental Quality*, 36, 935–942.
- Matheron, G. (1976). A simple substitute for conditional expectation: the disjunctive kriging. *Advanced Geostatistics in the Mining Industry NATO Advanced Study Institutes Series*, 24, 221–236.
- Mikkelsen, S. A. (1992). Current nitrate research in Denmark—background and practical application, nitrate and farming systems. *Aspects of Applied Biology*, 30, 29–44.
- Moraetis, D., Nikolaidis, N. P., Karatzas, G. P., Dokou, Z., Kalogerakis, N., Winkel, L. H. E., & Palaioianni-Bellou,

- A. (2012). Origin and mobility of hexavalent chromium in North-Eastern Attica, Greece. *Applied Geochemistry*, 27, 1170–1178.
- Panagiotakis, I., Dermatas, D., Vatsiris, C., Chrysochoou, M., Papassiopi, N., Xenidis, A., & Vaxevanidou, K. (2014). Forensic investigation of a chromium(VI) groundwater plume in Thiva, Greece. *Journal of Hazardous Materials*, 281, 27–34.
- Paritsis, S. N. (2001). *Management of the water resources of the Municipality of Malia*. Heraklion: OANAK (in Greek).
- Prasad, R. K., Singh, V. S., Krishnamacharyulu, S. K. G., & Banerjee, P. (2011). Application of drastic model and GIS: for assessing vulnerability in hard rock granitic aquifer. *Environmental Monitoring and Assessment*, 176, 143–155.
- Psarropoulou, E. T., & Karatzas, G. P. (2014). Pollution of Nitrates—contaminant transport in heterogeneous porous media: a case study of the coastal aquifer of Corinth. *Greece Global Nest Journal*, 16(1), 9–23.
- Rouhani, S., & Mayers, D. E. (1990). Problems in space-time kriging of geohydrological data. *Mathematical Geology*, 22(5), 611–623.
- Smedley, P. L., & Kinniburgh, D. G. (2002). A review of the source, behaviour and distribution of arsenic in natural waters. *Applied Geochemistry*, 17(5), 517–568.
- Varouchakis, E. A., Hristopulos, D. T., & Karatzas, G. P. (2012). Improving kriging of groundwater level data using nonlinear normalizing transformations—a field application. *Hydrological Sciences Journal*, 57(7), 1404–1419.
- Venteris, E. R., Basta, N. T., Bigham, J. M., & Rea, R. (2014). Modeling spatial patterns in soil arsenic to estimate natural baseline concentrations. *Journal of Environmental Quality*, 43, 936–946.
- Werner, A. D., Bakker, M., Post, V. E. A., Vandenbohede, A., Lu, C., Ataie-Ashtiani, B., Simmons, C. T., & Barry, A. (2013). Seawater intrusion processes, investigation, and management: recent advances and future challenges. *Advances in Water Resources*, 51, 3–26.
- Yates, S. R., Warrick, A. W., & Myers, D. E. (1986). Disjunctive kriging: 1. Overview of estimation and conditional probability. *Water Resources Research*, 22(5), 615–621.